Hindawi
Journal of Nanomaterials
Volume 2019, Article ID 4867909, 7 pages
https://doi.org/10.1155/2019/4867909

Research Article

Facile Hydrothermal Synthesis of Two-Dimensional Porous ZnO Nanosheets for Highly Sensitive Ethanol Sensor

Lai Van Duy,[1] Nguyen Hong Hanh,[1] Dang Ngoc Son,[1] Pham Tien Hung,[2] Chu Manh Hung,[1] Nguyen Van Duy,[1] Nguyen Duc Hoa,[1] and Nguyen Van Hieu[3,4]

[1]*International Training Institute for Materials Science (ITIMS), Hanoi University of Science and Technology (HUST), No. 1 Dai Co Viet, Hai Ba Trung, Hanoi, Vietnam*
[2]*Physics Faculty, Le Quy Don Technical University, No. 236 Hoang Quoc Viet street, Cau Giay District, Hanoi, Vietnam*
[3]*Faculty of Electrical and Electronic Engineering, Phenikaa Institute for Advanced Study (PIAS), Phenikaa University, Yen Nghia, Ha-Dong District, Hanoi 10000, Vietnam*
[4]*Phenikaa Research and Technology Institute (PRATI), A&A Green Phoenix Group, 167 Hoang Ngan, Hanoi 10000, Vietnam*

Correspondence should be addressed to Chu Manh Hung; mhchu@itims.edu.vn and Nguyen Duc Hoa; ndhoa@itims.edu.vn

Received 19 July 2019; Accepted 28 September 2019; Published 11 November 2019

Guest Editor: Fei Ke

Two-dimensional porous ZnO nanosheets were synthesized by a facile hydrothermal method for ethanol gas-sensing application. The morphology, composition, and structure of the synthesized materials were characterized by scanning electron microscopy, energy-dispersive X-ray spectroscopy, powder X-ray diffraction, and high-resolution transmission electron microcopy. Results showed that the synthesized ZnO materials were porous nanosheets with a smooth surface and a thickness of 100 nm and a large pore size of approximately 80 nm. The as-prepared nanosheets, which had high purity, high crystallinity, and good dispersion, were used to fabricate a gas sensor for ethanol gas detection at different operating temperatures. The porous ZnO nanosheet gas sensor exhibited a high response value of 21 toward 500 ppm ethanol at a working temperature of 400°C with a reversible and fast response to ethanol gas (12 s/231 s), indicating its potential application. We also discussed the plausible sensing mechanism of the porous ZnO nanosheets on the basis of the adopted ethanol sensor.

1. Introduction

Semiconductor metal oxide materials are drawing considerable attention for the development of sensors toward applications in numerous fields, such as air quality control, environmental monitor, and public safety from hazardous gases (e.g, NO_x, SO_x, CO_x, and H_2S) [1–6]. Substantial effort has also been devoted to the fabrication of metal oxide-based gas sensors for volatile organic compound (VOC) monitoring, such as benzene, toluene, acetone, methanol, and ethanol [7–11]. Studies have been attempting to adjust the properties of these gas-sensitive nanomaterials and to form new multifunctional nanostructures. Such nanostructures and/or quantum dots exhibit many attractive features, such as high chemical and thermal stability, large surface area, adjustable electronic state, quantum confinement, high electron mobility, and excellent catalytic properties [11, 12]. Different types of metal oxide nanostructures such as tin oxide (SnO_2), indium oxide (In_2O_3), zinc oxide (ZnO), tungsten trioxide (WO_3), cobalt oxide (Co_3O_4), nickel oxide (NiO), and titanium oxide (TiO_2) have been discovered for gas-sensing applications [4, 10, 13–17]. ZnO is a potential sensing material because of its outstanding properties; it is an environmentally friendly n-type semiconductor that has a direct and wide band gap of 3.37 eV, interenergy large exciton at room temperature (~60 meV), high thermal and chemical stability, high electronic mobility, ease of synthesis, low cost, high sensitivity to target gases, and large surface-to-volume ratio [10, 17, 18]. Extensive studies have been focused on the development of gas sensors based on ZnO nanostructures with various morphologies and composition for the detection of VOCs [19–21]. ZnO can reportedly be prepared on a large

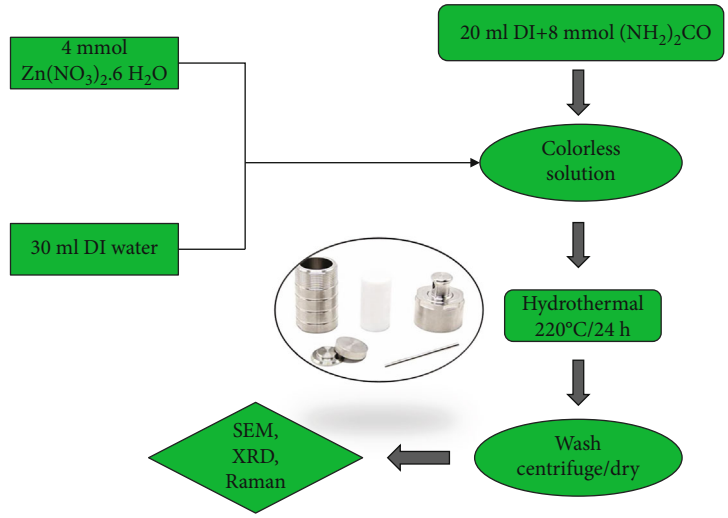

Figure 1: Hydrothermal synthesis process of porous ZnO nanosheets.

scale by using simple wet chemical glands as hydrothermal [17, 22], coprecipitation [23], sol-gel [24], electrospinning [25], thermal evaporation [26], and electrodeposition methods [27]. By utilizing the hydrothermal method, researchers can create a huge number of shapes and structures of this material [17, 22], which has a large surface-to-volume ratio, for use in different fields. However, an easy synthesis of porous ZnO nanosheets for gas sensor applications remains challenging.

In this study, we develop a simple hydrothermal method for synthesizing porous ZnO nanosheets for effective ethanol gas sensing in industry applications. Porous ZnO nanosheets possess a large specific surface area for gas adsorption because of its porous structure, thus showing superior sensitivity to ethanol.

2. Materials and Methods

Porous ZnO nanosheets were synthesized via a hydrothermal method followed by annealing at 600°C. The synthesis processes of the porous ZnO nanosheets are summarized in Figure 1, which was adapted from the literature [28, 29] with modification. In a typical synthesis, zinc nitrate hexahydrate ($Zn(NO_3)_2{\cdot}6H_2O$) (4 mmol) was dissolved in 30 mL deionized water. After this solution was stirred for 15 min, 20 mL urea (CH_4N_2O) (8 mmol) solution was added with further stirring for 15 min to adjust the pH to 5. The above turbid solution was transferred into a 100 mL Teflon-lined stainless steel autoclave for hydrothermal. The hydrothermal process was maintained at 220°C for 24 h. After being natural cooled to room temperature, the precipitate was centrifuged and washed with deionized water several times. Then, it was washed twice using an ethanol solution and collected by centrifugation at 4000 rpm. Finally, the white product was obtained and dried in an oven at 60°C for 24 h. The synthesized materials were characterized by field-emission scanning electron microscopy (SEM, JEOL 7600F), powder X-ray diffraction (XRD; Advance D8, Bruker), energy-dispersive X-ray spectroscopy (EDS), and high-resolution transmission electron microscopy (HRTEM, Tecnai G2F20S-TWIN, Philips). The synthesized porous ZnO nanosheets were then characterized sensing properties using a lab-made gas-sensing system [30].

3. Results and Discussion

Figures 2(a) and 2(b) show the SEM images of the grown material after it was calcined at 600°C for 2 h. The low-magnification SEM image (Figure 2(a)) demonstrates that the as-prepared products are composed of homogeneous nanosheets with porous structure. The high-magnification SEM image (Figure 2(b)) reveals that the synthesized nanosheets are nanosized porous architectures comprising sheet nanostructures with edge thicknesses of about 100 nm. Moreover, many small, round holes about 80 nm in diameter are evenly distributed on the surface. The large surface-to-volume ratio of nanosheets may provide large sites for gaseous-molecule adsorption, thereby enhancing the gas-sensing performance [4]. Herein, the homogenous nanosheets were obtained without using any surfactant, thus reducing the usage of chemicals. Zinc nitrate hexahydrate was used as a Zn^{2+} precursor, whereas the urea was utilized as media to control the solution pH. Urea was easily decomposed into NH_3 and HNCO during the hydrothermal process. Thus, it reacted with Zn^{2+} to form ZnO and generate the porous structure.

The crystal structure of the synthesized nanosheets was studied by XRD, and the data are shown in Figure 3(a). The main diffraction peaks are indexed to the (100), (002), (101), (102), (110), (103), (200), (112), (201), and (202) lattice planes of ZnO. All the diffraction peaks correspond to wurtzite ZnO (JCPDS card No. 36-1451) without other observable impurity characteristic peaks; therefore, high-purity ZnO can be obtained using the solvothermal method combined with calcination [10, 17]. The EDS analysis indicates the presence of Zn and O elements from the nanosheets

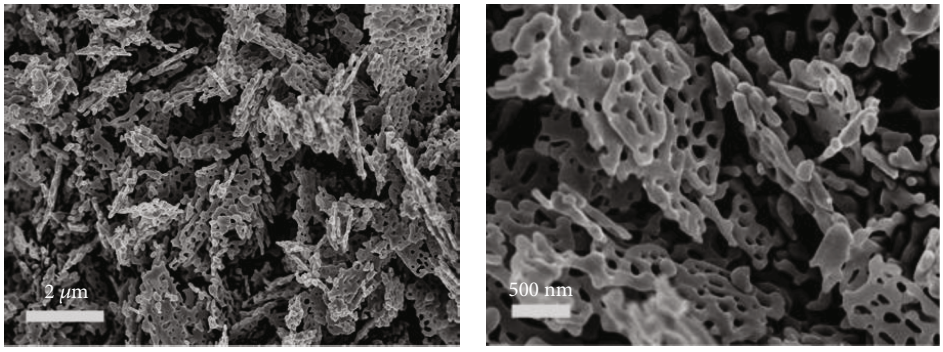

Figure 2: (a) Low- and (b) high-magnification SEM images of synthesized porous ZnO nanosheets.

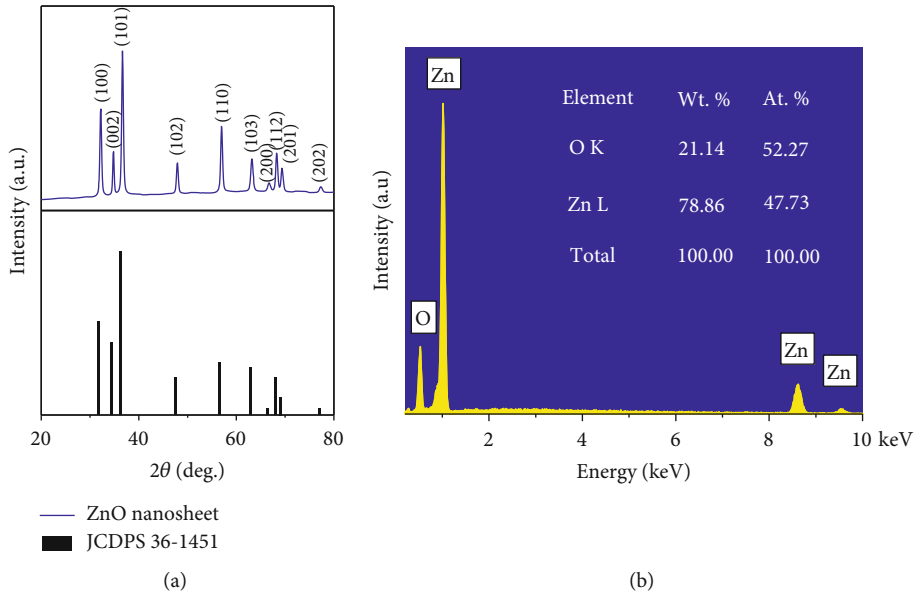

Figure 3: (a) XRD pattern and (b) EDS spectrum of the synthesized ZnO nanosheets annealed at 600°C for 2 h in air.

(Figure 3(b)). The synthesized nanosheets have no impurity and are thus of high quality. The O and Zn compositions estimated from the EDX analysis are 52.27 at.% and 47.74 at.%, respectively. This composition is approximately the stoichiometry ZnO [9].

The atomic structure of the porous ZnO nanosheets was investigated by HRTEM images and the selected area electron diffraction (SAED) patterns. Figure 4(a) shows a representative low magnification TEM image of the ZnO nanosheets taken on the red square region of the inset. It exhibits a smooth surface and the porous structure of the synthesized nanosheets, which confirm the results obtained from the SEM images. Figure 4(b) reveals a representative high magnification TEM image captured on the yellow square area of Figure 4(a). The image shows a well-defined lattice fringe separation with a lattice spacing of 0.52 nm, indicating a periodic ZnO lattice growth along the (001) plane. The inset of Figure 4(b) shows the corresponding SAED pattern obtained from the lattice fringes of the ZnO nanosheets, confirming that the synthesized ZnO has the single crystalline wurtzite structure growing along the [0001] direction [31].

The transient resistance versus time upon exposure to different concentrations of C_2H_5OH measured at temperatures ranging from 250°C to 400°C is shown in Figures 5(a)–5(d). Clearly, the sensor response value initially increases and then decreases with increased operating temperature. The maximum response for ethanol is 21 at the optimum operating temperature of 400°C. The sensor response S (R_a/R_g), as a function of C_2H_5OH concentrations measured at different temperatures, is shown in Figure 5(b).

At all measured temperatures, the sensor response increases with increased C_2H_5OH concentration in the measured range. At a given concentration, the sensor response increases with increased working temperature. However, increasing the working temperature requires a

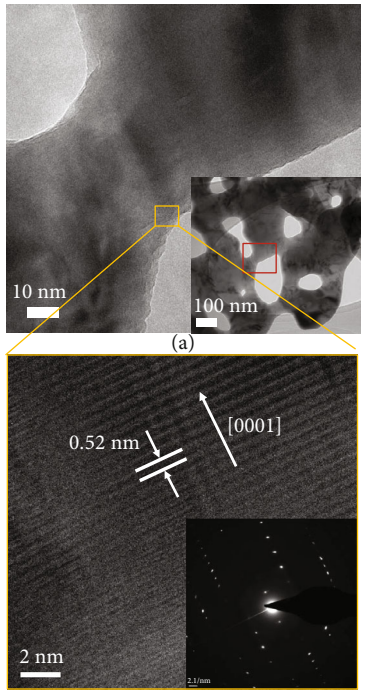

Figure 4: (a) Low and (b) high magnification TEM images of the porous ZnO nanosheet. Inset of (b) shows SAED pattern.

considerable amount of energy, which can damage microheaters. For practical applications, the power consumption of the device should be limited; thus, the sensor response at temperatures higher than 450°C did not need to be characterized.

The gas-sensing mechanism of metal oxide is based on the adsorption and desorption of gas molecules and chemical reactions on the surface of sensing materials [10, 32]. Herein, band diagrams of nanoporous ZnO nanosheet in air and in ethanol are shown in Figure 6 to explain the gas-sensing mechanism. ZnO is a well-known n-type conductor. When the sensor is exposed to air, oxygen molecules originating from the atmosphere adsorb onto the ZnO surface and then ionize to negative oxygen species via trapping free electrons from the conduction band, as shown in Equations (1)–(3).

$$O_2(\text{gas}) \longrightarrow O_2(\text{ads}) \quad (1)$$

$$O_2(\text{ads}) + e- \longrightarrow O^{2-}(\text{ads}) \quad (2)$$

$$O^{2-}(\text{ads}) + e- \longrightarrow 2O^{-}(\text{ads}) \quad (3)$$

When reductive C_2H_5OH gas vapour approaches to the sensor, it reacts with the adsorbed oxygen species on the ZnO sheets. Consequently, the captured electrons will be released to the ZnO, ultimately decreasing the surface depletion layer and the sensor resistance. The reaction process

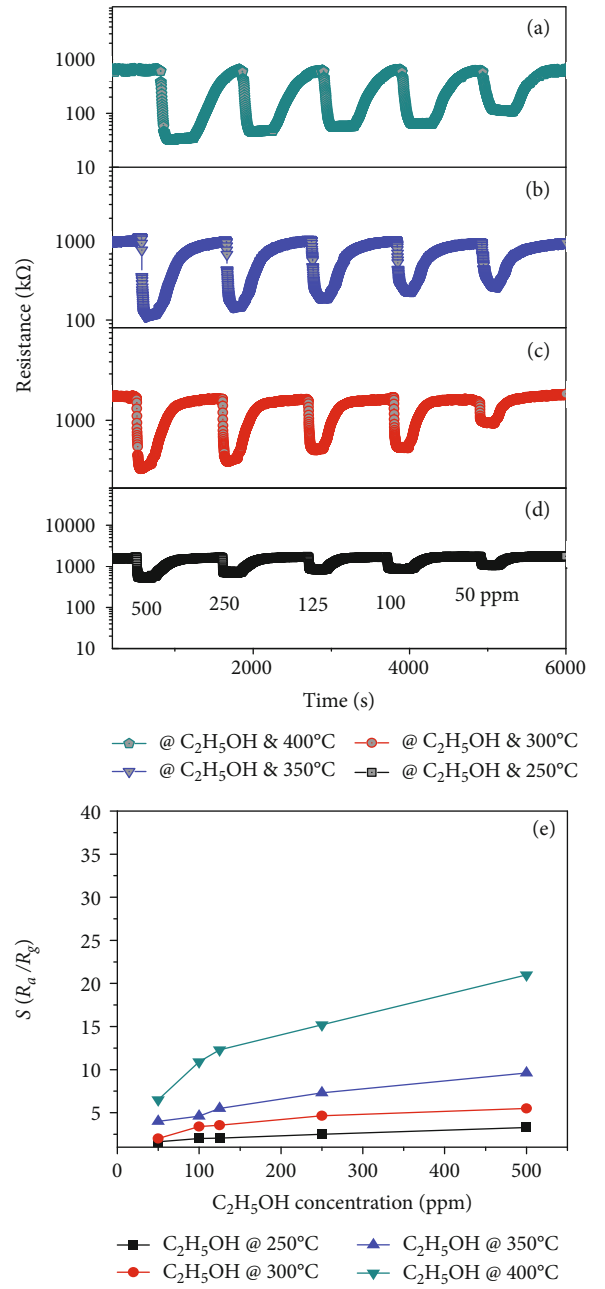

Figure 5: C_2H_5OH sensing characteristics of porous ZnO nanosheets measured at different operating temperatures: transient resistance versus time upon exposure to different C_2H_5OH concentrations at 450°C (a), 400°C (b), 350°C (c), and 250°C (d); (e) gas response as a function of C_2H_5OH concentration.

between the surface-adsorbed oxygen species and ethanol is described by Equations (4)–(6).

$$C_2H_5OH + 3O_2^{-} \longrightarrow 2CO_2 + 3H_2O + 3e^{-} \quad (4)$$

$$C_2H_5OH + 6O^{-} \longrightarrow 2CO_2 + 3H_2O + 6e^{-} \quad (5)$$

$$C_2H_5OH + 6O^{-} \longrightarrow 2CO_2 + 3H_2O + 12e^{-} \quad (6)$$

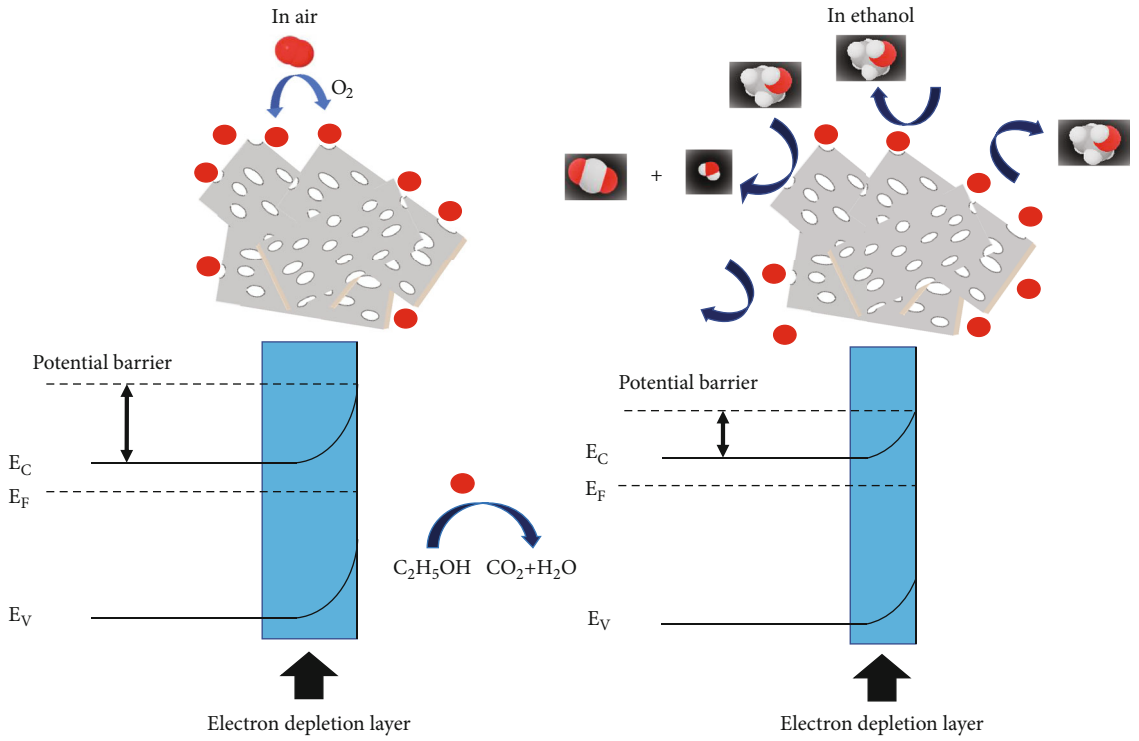

Figure 6: Schematic of the C_2H_5OH gas-sensing mechanism of the nanoporous ZnO.

Table 1: Comparison of different ZnO nanosheet-based VOC gas sensors.

Materials	Gas	C (ppm)	Response	T (°C)	Ref.
ZnO NPs	Ethanol	100	5	350	[33]
Au-ZnO NWs	Ethanol	50	7	325	[34]
ZnO NFs	Ethanol	100	6	340	[35]
ZnO NFs	Acetone	100	4	360	[35]
Sn doped ZnO NSs	Acetone	200	5.55	320	[36]
ZnO nanoplate	Chlorobenzene	100	2	400	[37]
Porous ZnO NSs	Ethanol	100	11	400	This work
Porous ZnO NSs	Ethanol	500	21	400	This work

Given the porous structure of the nanosheets, gas molecules can easily adsorb onto the total surface of the ZnO nanosheet and significantly change the depletion region, thus maximizing the sensing performance [13].

Comparative results of the fabricated sensor with those in other reports are summarized in Table 1. The porous ZnO nanosheets produced the highest response value to ethanol, followed by the Au-modified ZnO nanowires, ZnO nanofibers, and ZnO nanoparticles. The sensor also showed a higher response value for ethanol gas compared with acetone and chlorobenzene. However, the porous ZnO nanosheets operated at a relatively higher working temperature. The high working temperature and low sensitivity of the sensor limited its potential application. Therefore, the controlled synthesis of highly sensitive ethanol sensors that operate at low temperatures is mandatory for future sensor applications.

The gas selectivity of the porous ZnO nanosheet sensor was tested to various gases, namely, CH_3OH, $C_6H_5CH_3$, and NH_3, at 400°C with a gas concentration of 500 ppm, as shown in Figure 7(a). The data show that the response of the nanoporous ZnO sensor to 500 ppm C_2H_5OH is much higher than that of the sensors to other gases at the same concentration and working temperature. This finding indicates good selectivity of the porous ZnO nanosheet sensor to C_2H_5OH gas. Figure 7(b) reveals the short-term stability of the porous ZnO nanosheet sensor with 10 response/recovery cycles to 125 ppm C_2H_5OH at 400°C. The sensor can noticeably maintain its initial response amplitude with 10 continuous response/recovery cycles. These results indicate that the sensor has good selectivity, reproducibility, and short-term stability, which are important characteristics of gas sensors for practical applications.

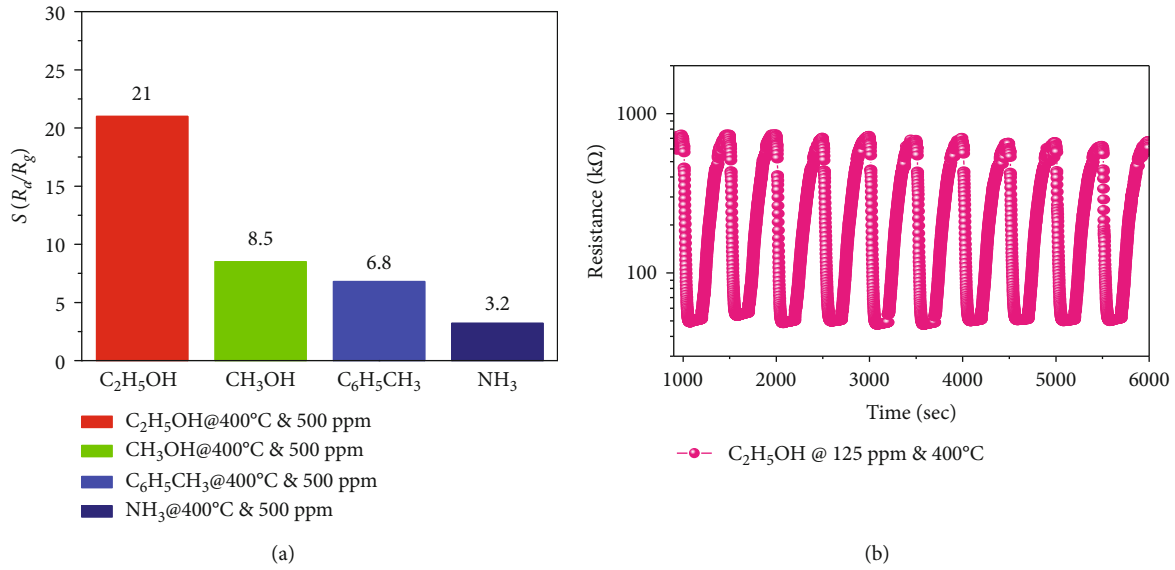

FIGURE 7: (a) Selectivity to various gases at 400°C and stability at 125 ppm C_2H_5OH gas at 400°C of the nanoporous ZnO nanosheet-based sensors.

4. Conclusions

We introduced an easy and scalable hydrothermal synthesis of nanoporous ZnO nanosheets for effective C_2H_5OH gas-sensing applications. The obtained porous nanosheets performed good crystallinity and dispersing levels. The mean thickness of the ZnO nanosheets is approximately 100 nm, and the pore size is about 80 nm. The obtained nanoporous ZnO nanosheets exhibited excellent gas-sensing properties to ethanol in terms of high and fast response and recovery times. The results show that nanoporous ZnO nanosheets can be a potential material for high-performance ethanol gas sensing.

Data Availability

The data used to support the findings of this study are included within the article.

Conflicts of Interest

The authors declare that there is no conflict of interest regarding the publication of this paper.

Acknowledgments

This research was funded by the Vietnam National Foundation for Science and Technology Development (NAFOSTED) under grant number 103.02-2017.15. We would like to thank Prof. Young-Woo Heo (Kyungpook National University) for his help with TEM measurement.

References

[1] P. Van Tong, N. D. Hoa, H. T. Nha, N. Van Duy, C. M. Hung, and N. Van Hieu, "SO_2 and H_2S sensing properties of hydrothermally synthesized CuO nanoplates," *Journal of Electronic Materials*, vol. 47, no. 12, pp. 7170–7178, 2018.

[2] C. M. Hung, D. T. T. Le, and N. Van Hieu, "On-chip growth of semiconductor metal oxide nanowires for gas sensors: a review," *Journal of Science: Advanced Materials and Devices*, vol. 2, no. 3, pp. 263–285, 2017.

[3] T. M. Ngoc, N. Van Duy, N. Duc Hoa, C. Manh Hung, H. Nguyen, and N. Van Hieu, "Effective design and fabrication of low-power-consumption self-heated SnO_2 nanowire sensors for reducing gases," *Sensors and Actuators B: Chemical*, vol. 295, pp. 144–152, 2019.

[4] N. D. Hoa, C. M. Hung, N. Van Duy, and N. Van Hieu, "Nanoporous and crystal evolution in nickel oxide nanosheets for enhanced gas- sensing performance," *Sensors and Actuators B: Chemical*, vol. 273, pp. 784–793, 2018.

[5] N. D. Hoa, N. V. Duy, S. A. el-Safty, and N. V. Hieu, "Meso-/nanoporous semiconducting metal oxides for gas sensor applications," *Journal of Nanomaterials*, vol. 2015, 14 pages, 2015.

[6] X. Li, X. Li, N. Chen et al., "CuO-In_2O_3 Core-Shell Nanowire Based Chemical Gas Sensors," *Journal of Nanomaterials*, vol. 2014, Article ID 973156, 7 pages, 2014.

[7] C. Su, L. Zhang, Y. Han et al., "Glucose-assisted synthesis of hierarchical flower-like Co_3O_4 nanostructures assembled by porous nanosheets for enhanced acetone sensing," *Sensors and Actuators B: Chemical*, vol. 288, pp. 699–706, 2019.

[8] X. Liu, K. Zhao, X. Sun, X. Duan, C. Zhang, and X. Xu, "Electrochemical sensor to environmental pollutant of acetone based on Pd- loaded on mesoporous In_2O_3 architecture," *Sensors and Actuators B: Chemical*, vol. 290, pp. 217–225, 2019.

[9] X. Wang, F. Chen, M. Yang et al., "Dispersed WO_3 nanoparticles with porous nanostructure for ultrafast toluene sensing," *Sensors and Actuators B: Chemical*, vol. 289, pp. 195–206, 2019.

[10] C. T. Quy, N. X. Thai, N. D. Hoa et al., "C_2H_5OH and NO2sensing properties of ZnO nanostructures: correlation between

crystal size, defect level and sensing performance," *RSC Advances*, vol. 8, no. 10, pp. 5629–5639, 2018.

[11] C. Su, L. Zhang, Y. Han et al., "Controllable synthesis of crescent-shaped porous NiO nanoplates for conductometric ethanol gas sensors," *Sensors and Actuators B: Chemical*, vol. 296, p. 126642, 2019.

[12] J. Zhu, F. Zhu, X. Yue et al., "Waste utilization of synthetic carbon quantum dots based on tea and peanut shell," *Journal of Nanomaterials*, vol. 2019, 7 pages, 2019.

[13] T. T. Le Dang, M. Tonezzer, and V. H. Nguyen, "Hydrothermal growth and hydrogen selective sensing of nickel oxide nanowires," *Journal of Nanomaterials*, vol. 2015, Article ID 785856, 8 pages, 2015.

[14] P. Bindra and A. Hazra, "Selective detection of organic vapors using TiO_2 nanotubes based single sensor at room temperature," *Sensors and Actuators B: Chemical*, vol. 290, pp. 684–690, 2019.

[15] D. Zhang, Y. Fan, G. Li et al., "Highly sensitive BTEX sensors based on hexagonal WO_3 nanosheets," *Sensors and Actuators B: Chemical*, vol. 293, pp. 23–30, 2019.

[16] P. Van Tong, N. D. Hoa, N. Van Duy, V. Van Quang, N. T. Lam, and N. Van Hieu, "In-situ decoration of Pd nanocrystals on crystalline mesoporous NiO nanosheets for effective hydrogen gas sensors," *International Journal of Hydrogen Energy*, vol. 38, no. 27, pp. 12090–12100, 2013.

[17] V. T. Duoc, D. T. T. Le, N. D. Hoa et al., "New design of ZnO nanorod- and nanowire-based NO_2 room-temperature sensors prepared by hydrothermal method," *Journal of Nanomaterials*, vol. 2019, Article ID 6821937, 9 pages, 2019.

[18] M. L. M. Napi, S. M. Sultan, R. Ismail, M. K. Ahmad, and G. M. T. Chai, "Optimization of a hydrothermal growth process for low resistance 1D fluorine-doped zinc oxide nanostructures," *Journal of Nanomaterials*, vol. 2019, Article ID 4574507, 10 pages, 2019.

[19] N. D. Khoang, D. D. Trung, N. Van Duy, N. D. Hoa, and N. Van Hieu, "Design of SnO_2/ZnO hierarchical nanostructures for enhanced ethanol gas-sensing performance," *Sensors and Actuators B: Chemical*, vol. 174, pp. 594–601, 2012.

[20] S.-M. Li, L.-X. Zhang, M.-Y. Zhu et al., "Acetone sensing of ZnO nanosheets synthesized using room-temperature precipitation," *Sensors and Actuators B: Chemical*, vol. 249, pp. 611–623, 2017.

[21] S. Agarwal, P. Rai, E. N. Gatell et al., "Gas sensing properties of ZnO nanostructures (flowers/rods) synthesized by hydrothermal method," *Sensors and Actuators B: Chemical*, vol. 292, pp. 24–31, 2019.

[22] G. Amin, M. H. Asif, A. Zainelabdin, S. Zaman, O. Nur, and M. Willander, "Influence of pH, precursor concentration, growth time, and temperature on the morphology of ZnO nanostructures grown by the hydrothermal method," *Journal of Nanomaterials*, vol. 2011, Article ID 269692, 9 pages, 2011.

[23] M. El-Hilo, A. A. Dakhel, and Z. J. Yacoob, "Magnetic interactions in Co^{2+} doped ZnO synthesised by co-precipitation method: efficient effect of hydrogenation on the long-range ferromagnetic order," *Journal of Magnetism and Magnetic Materials*, vol. 482, pp. 125–134, 2019.

[24] Y. Zeng, L. Qiao, Y. Bing et al., "Development of microstructure CO sensor based on hierarchically porous ZnO nanosheet thin films," *Sensors and Actuators B: Chemical*, vol. 173, pp. 897–902, 2012.

[25] J.-H. Kim, A. Mirzaei, H. W. Kim, P. Wu, and S. S. Kim, "Design of supersensitive and selective ZnO-nanofiber-based sensors for H_2 gas sensing by electron-beam irradiation," *Sensors and Actuators B: Chemical*, vol. 293, pp. 210–223, 2019.

[26] C. M. Hung, H. V. Phuong, N. Van Duy, N. D. Hoa, and N. Van Hieu, "Comparative effects of synthesis parameters on the NO_2 gas-sensing performance of on-chip grown ZnO and Zn_2SnO_4 nanowire sensors," *Journal of Alloys and Compounds*, vol. 765, pp. 1237–1242, 2018.

[27] C. Wang, Z.-G. Wang, R. Xi et al., "In situ synthesis of flower-like ZnO on GaN using electrodeposition and its application as ethanol gas sensor at room temperature," *Sensors and Actuators B: Chemical*, vol. 292, pp. 270–276, 2019.

[28] Z. Feng, Y. Ma, V. Natarajan, Q. Zhao, X. Ma, and J. Zhan, "In-situ generation of highly dispersed Au nanoparticles on porous ZnO nanoplates via ion exchange from hydrozincite for VOCs gas sensing," *Sensors and Actuators B: Chemical*, vol. 255, pp. 884–890, 2018.

[29] Y. Xiao, L. Lu, A. Zhang et al., "Highly enhanced acetone sensing performances of porous and single crystalline ZnO nanosheets: high percentage of exposed (100) facets working together with surface modification with Pd nanoparticles," *ACS Applied Materials & Interfaces*, vol. 4, no. 8, pp. 3797–3804, 2012.

[30] K. Nguyen, C. M. Hung, T. M. Ngoc et al., "Low-temperature prototype hydrogen sensors using Pd-decorated SnO_2 nanowires for exhaled breath applications," *Sensors and Actuators B: Chemical*, vol. 253, pp. 156–163, 2017.

[31] W. L. Ong, H. Huang, J. Xiao, K. Zeng, and G. W. Ho, "Tuning of multifunctional cu-doped ZnO films and nanowires for enhanced piezo/ferroelectric-like and gas/photoresponse properties," *Nanoscale*, vol. 6, no. 3, pp. 1680–1690, 2014.

[32] X. Xing, Y. Yang, Z. Yan et al., "CdO-Ag-ZnO nanocomposites with hierarchically porous structure for effective VOCs gas-sensing properties," *Ceramics International*, vol. 45, no. 4, pp. 4322–4334, 2019.

[33] L. Zhu, Y. Li, and W. Zeng, "Hydrothermal synthesis of hierarchical flower-like ZnO nanostructure and its enhanced ethanol gas-sensing properties," *Applied Surface Science*, vol. 427, pp. 281–287, 2018.

[34] N. S. Ramgir, M. Kaur, P. K. Sharma et al., "Ethanol sensing properties of pure and Au modified ZnO nanowires," *Sensors and Actuators B: Chemical*, vol. 187, pp. 313–318, 2013.

[35] L. Liu, S. Li, J. Zhuang et al., "Improved selective acetone sensing properties of Co-doped ZnO nanofibers by electrospinning," *Sensors and Actuators B: Chemical*, vol. 155, no. 2, pp. 782–788, 2011.

[36] Y. Al-Hadeethi, A. Umar, S. H. Al-Heniti et al., "2D Sn-doped ZnO ultrathin nanosheet networks for enhanced acetone gas sensing application," *Ceramics International*, vol. 43, no. 2, pp. 2418–2423, 2017.

[37] Z. Jing and J. Zhan, "Fabrication and Gas-Sensing Properties of Porous ZnO Nanoplates," *Advanced Materials*, vol. 20, no. 23, pp. 4547–4551, 2008.